KEK Preprint 2000-82
BELLE-CONF-0013
August 2000
H

Measurements of exclusive decays $\bar{B}^0 \to D^+ \ell^- \bar{\nu}$ and $\bar{B}^0 \to D^{*+} \ell^- \bar{\nu}$ at Belle

The Belle Collaboration

Submitted to the XXXth International Conference on High Energy Physics, July-August 2000, Osaka, Japan.

High Energy Accelerator Research Organization (KEK)

KEK Reports are available from:

Information Resources Division
High Energy Accelerator Research Organization (KEK)
1-1 Oho, Tsukuba-shi
Ibaraki-ken, 305-0801
JAPAN

Phone: +81-298-64-5137
Fax: +81-298-64-4604
E-mail: adm-jouhoushiryou1@ccgemail.kek.jp
Internet: http://www.kek.jp

BELLE-CONF-0013
Parallel Session: PA-07
Plenary Session: PL-01b

Measurements of exclusive decays $\bar{B}^0 \to D^+\ell^-\bar{\nu}$ and $\bar{B}^0 \to D^{*+}\ell^-\bar{\nu}$ at Belle

The Belle Collaboration

Abstract

We present preliminary measurements of branching fractions for the exclusive B semileptonic decays, $\bar{B}^0 \to D^+\ell^-\bar{\nu}$ and $\bar{B}^0 \to D^{*+}\ell^-\bar{\nu}$. The data sample corresponds to 2.7 fb^{-1} of integrated luminosity obtained in asymmetric e^+e^- collisions at $\sqrt{s} = 10.58$ GeV at the KEKB collider and recorded with the Belle detector. The following exclusive B semileptonic branching fractions are obtained: $\mathcal{B}(\bar{B}^0 \to D^+\ell^-\bar{\nu}) = 2.07 \pm 0.21 \pm 0.31$ (%) and $\mathcal{B}(\bar{B}^0 \to D^{*+}\ell^-\bar{\nu}) = 4.74 \pm 0.25 \pm 0.51$ (%).

Typeset using REVTEX

A. Abashian[44], K. Abe[8], K. Abe[36], I. Adachi[8], Byoung Sup Ahn[14], H. Aihara[37], M. Akatsu[19], G. Alimonti[7], K. Aoki[8], K. Asai[20], M. Asai[9], Y. Asano[42], T. Aso[41], V. Aulchenko[2], T. Aushev[12], A. M. Bakich[33], E. Banas[15], S. Behari[8], P. K. Behera[43], D. Beiline[2], A. Bondar[2], A. Bozek[15], T. E. Browder[7], B. C. K. Casey[7], P. Chang[23], Y. Chao[23], B. G. Cheon[32], S.-K. Choi[6], Y. Choi[32], Y. Doi[8], J. Dragic[17], A. Drutskoy[12], S. Eidelman[2], Y. Enari[19], R. Enomoto[8,10], C. W. Everton[17], F. Fang[7], H. Fujii[8], K. Fujimoto[19], Y. Fujita[8], C. Fukunaga[39], M. Fukushima[10], A. Garmash[2,8], A. Gordon[17], K. Gotow[44], H. Guler[7], R. Guo[21], J. Haba[8], T. Haji[4], H. Hamasaki[8], K. Hanagaki[29], F. Handa[36], K. Hara[27], T. Hara[27], T. Haruyama[8], N. C. Hastings[17], K. Hayashi[8], H. Hayashii[20], M. Hazumi[27], E. M. Heenan[17], Y. Higashi[8], Y. Higasino[19], I. Higuchi[36], T. Higuchi[37], T. Hirai[38], H. Hirano[40], M. Hirose[19], T. Hojo[27], Y. Hoshi[35], K. Hoshina[40], W.-S. Hou[23], S.-C. Hsu[23], H.-C. Huang[23], Y.-C. Huang[21], S. Ichizawa[38], Y. Igarashi[8], T. Iijima[8], H. Ikeda[8], K. Ikeda[20], K. Inami[19], Y. Inoue[26], A. Ishikawa[19], R. Itoh[8], G. Iwai[25], M. Iwai[8], H. Iwasaki[8], Y. Iwasaki[8], D. J. Jackson[27], P. Jalocha[15], H. K. Jang[31], M. Jones[7], R. Kagan[12], H. Kakuno[38], J. Kaneko[38], J. H. Kang[45], J. S. Kang[14], P. Kapusta[15], K. Kasami[8], N. Katayama[8], H. Kawai[3], M. Kawai[8], N. Kawamura[1], T. Kawasaki[25], H. Kichimi[8], D. W. Kim[32], Heejong Kim[45], H. J. Kim[45], Hyunwoo Kim[14], S. K. Kim[31], K. Kinoshita[5], S. Kobayashi[30], S. Koike[8], Y. Kondo[8], H. Konishi[40], K. Korotushenko[29], P. Krokovny[2], R. Kulasiri[5], S. Kumar[28], T. Kuniya[30], E. Kurihara[3], A. Kuzmin[2], Y.-J. Kwon[45], M. H. Lee[8], S. H. Lee[31], C. Leonidopoulos[29], H.-B. Li[11], R.-S. Lu[23], Y. Makida[8], A. Manabe[8], D. Marlow[29], T. Matsubara[37], T. Matsuda[8], S. Matsui[19], S. Matsumoto[4], T. Matsumoto[19], K. Misono[19], K. Miyabayashi[20], H. Miyake[27], H. Miyata[25], L. C. Moffitt[17], G. R. Moloney[17], G. F. Moorhead[17], N. Morgan[44], S. Mori[42], T. Mori[4], A. Murakami[30], T. Nagamine[36], Y. Nagasaka[18], Y. Nagashima[27], T. Nakadaira[37], T. Nakamura[38], E. Nakano[26], M. Nakao[8], H. Nakazawa[4], J. W. Nam[32], S. Narita[36], Z. Natkaniec[15], K. Neichi[35], S. Nishida[16], O. Nitoh[40], S. Noguchi[20], T. Nozaki[8], S. Ogawa[34], R. Ohkubo[8], T. Ohshima[19], Y. Ohshima[38], T. Okabe[19], T. Okazaki[20], S. Okuno[13], S. L. Olsen[7], W. Ostrowicz[15], H. Ozaki[8], P. Pakhlov[12], H. Palka[15], C. S. Park[31], C. W. Park[14], H. Park[14], L. S. Peak[33], M. Peters[7], L. E. Piilonen[44], E. Prebys[29], J. Raaf[5], J. L. Rodriguez[7], N. Root[2], M. Rozanska[15], K. Rybicki[15], J. Ryuko[27], H. Sagawa[8], Y. Sakai[8], H. Sakamoto[16], H. Sakaue[26], M. Satapathy[43], N. Sato[8], A. Satpathy[8,5], S. Schrenk[44], S. Semenov[12], Y. Settai[4], M. E. Sevior[17], H. Shibuya[34], B. Shwartz[2], A. Sidorov[2], V. Sidorov[2], S. Stanič[42], A. Sugi[19], A. Sugiyama[19], K. Sumisawa[27], T. Sumiyoshi[8], J. Suzuki[8], J.-I. Suzuki[8], K. Suzuki[3], S. Suzuki[19], S. Y. Suzuki[8], S. K. Swain[7], H. Tajima[37], T. Takahashi[26], F. Takasaki[8], M. Takita[27], K. Tamai[8], N. Tamura[25], J. Tanaka[37], M. Tanaka[8], Y. Tanaka[18], G. N. Taylor[17], Y. Teramoto[26], M. Tomoto[19], T. Tomura[37], S. N. Tovey[17], K. Trabelsi[7], T. Tsuboyama[8], Y. Tsujita[42], T. Tsukamoto[8], T. Tsukamoto[30], S. Uehara[8], K. Ueno[23], N. Ujiie[8], Y. Unno[3], S. Uno[8], Y. Ushiroda[16], Y. Usov[2], S. E. Vahsen[29], G. Varner[7], K. E. Varvell[33], C. C. Wang[23], C. H. Wang[22], M.-Z. Wang[23], T.-J. Wang[11], Y. Watanabe[38], E. Won[31], B. D. Yabsley[8], Y. Yamada[8], M. Yamaga[36], A. Yamaguchi[36], H. Yamaguchi[8], H. Yamamoto[7], H. Yamaoka[8], Y. Yamaoka[8], Y. Yamashita[24], M. Yamauchi[8], S. Yanaka[38], M. Yokoyama[37], K. Yoshida[19], Y. Yusa[36], H. Yuta[1], C.-C. Zhang[11], H. W. Zhao[8], Y. Zheng[7], V. Zhilich[2], and D. Žontar[42]

[1]Aomori University, Aomori

[2]Budker Institute of Nuclear Physics, Novosibirsk
[3]Chiba University, Chiba
[4]Chuo University, Tokyo
[5]University of Cincinnati, Cincinnati, OH
[6]Gyeongsang National University, Chinju
[7]University of Hawaii, Honolulu HI
[8]High Energy Accelerator Research Organization (KEK), Tsukuba
[9]Hiroshima Institute of Technology, Hiroshima
[10]Institute for Cosmic Ray Research, University of Tokyo, Tokyo
[11]Institute of High Energy Physics, Chinese Academy of Sciences, Beijing
[12]Institute for Theoretical and Experimental Physics, Moscow
[13]Kanagawa University, Yokohama
[14]Korea University, Seoul
[15]H. Niewodniczanski Institute of Nuclear Physics, Krakow
[16]Kyoto University, Kyoto
[17]University of Melbourne, Victoria
[18]Nagasaki Institute of Applied Science, Nagasaki
[19]Nagoya University, Nagoya
[20]Nara Women's University, Nara
[21]National Kaohsiung Normal University, Kaohsiung
[22]National Lien-Ho Institute of Technology, Miao Li
[23]National Taiwan University, Taipei
[24]Nihon Dental College, Niigata
[25]Niigata University, Niigata
[26]Osaka City University, Osaka
[27]Osaka University, Osaka
[28]Panjab University, Chandigarh
[29]Princeton University, Princeton NJ
[30]Saga University, Saga
[31]Seoul National University, Seoul
[32]Sungkyunkwan University, Suwon
[33]University of Sydney, Sydney NSW
[34]Toho University, Funabashi
[35]Tohoku Gakuin University, Tagajo
[36]Tohoku University, Sendai
[37]University of Tokyo, Tokyo
[38]Tokyo Institute of Technology, Tokyo
[39]Tokyo Metropolitan University, Tokyo
[40]Tokyo University of Agriculture and Technology, Tokyo
[41]Toyama National College of Maritime Technology, Toyama
[42]University of Tsukuba, Tsukuba
[43]Utkal University, Bhubaneswer
[44]Virginia Polytechnic Institute and State University, Blacksburg VA
[45]Yonsei University, Seoul

I. INTRODUCTION

In the Standard Model (SM) of electroweak interactions, the elements of the Cabibbo-Kobayashi-Maskawa (CKM) quark mixing matrix [1] are constrained only by unitarity. Therefore, experimentally measuring the precise values of the CKM matrix elements is important for understanding the phenomenology of weak interactions. In particular, it is important to test the SM description of CP violation in B decay.

The exclusive semileptonic decays $\bar{B}^0 \to D^+\ell^-\bar{\nu}$ and $\bar{B}^0 \to D^{*+}\ell^-\bar{\nu}$ are among the cleanest modes to measure the CKM matrix element $|V_{cb}|$ when interpreted in the framework of heavy quark effective theory (HQET) [2]. The $\bar{B}^0 \to D^+\ell^-\bar{\nu}$ decay is preferred to $B^- \to D^0\ell^-\nu$ because it has much less feed-down background from excited charm meson states. For $\bar{B}^0 \to D^{*+}\ell^-\bar{\nu}$, the signal is very clean using the $D^* - D$ mass-difference. Moreover, since the branching ratio is large, the statistical uncertainty is relatively small.

In this paper, we present preliminary measurements of the branching ratios for the exclusive B semileptonic decays, $\bar{B}^0 \to D^+\ell^-\bar{\nu}$ and $\bar{B}^0 \to D^{*+}\ell^-\bar{\nu}$, using a data sample obtained in asymmetric e^+e^- collisions at $\sqrt{s} = 10.58$ GeV at the KEKB collider [3] and recorded with the Belle detector [4]. With good particle identification and vertexing capability as well as a potential for very large statistics, the Belle experiment will improve the precision in the measurements of $\bar{B}^0 \to D^+\ell^-\bar{\nu}$ and $\bar{B}^0 \to D^{*+}\ell^-\bar{\nu}$, and eventually of $|V_{cb}|$.

II. BELLE DETECTOR

The event sample used for this study corresponds to an integrated luminosity of 2.7 fb^{-1} accumulated at the $\Upsilon(4S)$ resonance and recorded in the Belle detector at the KEKB e^+e^- collider. An event sample of 0.6 fb^{-1} integrated luminosity taken 60 MeV below the $\Upsilon(4S)$ resonance was also used as a control sample to check the continuum background estimation.

The Belle detector is a large solid-angle spectrometer based on a 1.5 T superconducting solenoid magnet. Tracking and momentum measurements of charged particles are performed with a 3-layer double-sided silicon vertex detector (SVD) [5] and a cylindrical drift chamber (CDC) [6]. The charged particle acceptance covers the laboratory polar angle range between $\theta = 17°$ and $150°$ corresponding to about 90% of the full solid angle in the center-of-mass frame. A Kalman filtering technique is used to determine the optimal track parameters.

Hadron identification is provided by specific ionization (dE/dx) measurements in the CDC, Cherenkov threshold measurements in the aerogel Cherenkov counters (ACC) [7], and a cylindrical array of 128 time-of-flight scintillation counters (TOF) [8]. This provides separation of kaons and pions in the momentum range up to 4 GeV/c. To determine the hadron identification efficiency and fake rates, we use kinematically selected $D^{*+} \to D^0\pi^+$ and subsequent $D^0 \to K^-\pi^+$ decays.

Electrons are identified by using a likelihood function that includes the following information: the ratio of energy measured by electromagnetic calorimeter (ECL, consisting of 8736 CsI crystals [9]) and the momentum determined by the CDC, the ratio of energy deposited in 9 crystals and 25 crystals around the cluster centroid at the calorimeter, close matching between the extrapolated track position and the cluster position, dE/dx measured by the CDC, light yield in the ACC and the TOF information. Muons are identified with a resistive plate chamber system interspersed in the iron return yoke of the magnet (KLM)

[10] by comparing the calculated track range with the measured range, and by determining the χ^2 of the KLM hits with respect to the track extrapolated with Kalman filtering.

III. EVENT SELECTION AND ANALYSIS PROCEDURE

A. Background sources

In both the $\bar{B}^0 \to D^+\ell^-\bar{\nu}$ and $\bar{B}^0 \to D^{*+}\ell^-\bar{\nu}$ analyses, the background sources fall into five categories: combinatoric, correlated, uncorrelated, continuum and misidentified lepton. The event selection procedure is designed to suppress these backgrounds effectively.

Combinatoric Background The dominant background in this analysis is the combinatoric background in $D^{(*)+}$ reconstruction. The magnitudes of combinatoric backgrounds are estimated using sideband data: the sideband in $m(K^-\pi^+\pi^+)$ is used for $\bar{B}^0 \to D^+\ell^-\bar{\nu}$ and the sideband of $m(K^-\pi^+)$ and the sideband of the mass difference $m(K^-\pi^+\pi^+) - m(K^-\pi^+)$ are used for the $D^*\ell\nu$ analysis.

Correlated Background If a $D^{(*)+}$ and a lepton have the same parent B, but do not come from the signal decay $\bar{B}^0 \to D^{(*)+}\ell^-\nu$, the event is classified as a correlated background. Processes such as $\bar{B}^0 \to D^{**}\ell\nu$ and $D^{(*)}\pi\ell\nu$ contribute to this source. The decay $\bar{B}^0 \to D^{*+}\ell^-\nu$ is also a correlated background source for $B \to D^+\ell\nu$. To estimate this background, we use a Monte Carlo (MC) sample which is based on the ISGW2 model [12].

Uncorrelated Background Uncorrelated backgrounds are events with a real $D^{(*)}$ from the decay of one B meson and a real lepton from the opposite B. We also use MC simulation to estimate this background. Due to the charge correlation with the $D^{(*)}$, the lepton in this background is usually from a secondary decay, and is somewhat suppressed by the momentum cut required for leptons.

Misidentified lepton background In this case, a hadron track is misidentified as a lepton. Its magnitude is estimated from real data: we treat each hadron candidate track as if it were a signal lepton and weight its contribution according to the misidentification probability measured using kinematically identified hadron tracks in real data.

Continuum background The $e^+e^- \to q\bar{q}$ continuum background is estimated using MC continuum events. We also check that this estimate is statistically consistent with off-resonance data.

B. The $\bar{B}^0 \to D^+\ell^-\bar{\nu}$ mode

We analyze the decay mode $\bar{B}^0 \to D^+\ell^-\bar{\nu}$, where the D^+ subsequently decays to $K^-\pi^+\pi^+$. Charge-conjugate modes are implied throughout this paper. The analysis of this decay mode is based on the neutrino reconstruction method, which exploits the hermeticity of the detector and near zero value of neutrino mass. This method was originally developed by the CLEO Collaboration for the measurement of $B \to \pi\ell\nu$ and $\rho(\omega)\ell\nu$ decays [13]. In each event, we measure the missing energy, $E_{\rm miss}$, and missing momentum, $\vec{p}_{\rm miss}$ and require:

$$M^2_{\rm miss} = E^2_{\rm miss} - p^2_{\rm miss} \approx 0. \qquad (1)$$

In principle, this selects events where there is only one undetected particle in the event and that missing particle is the neutrino. Usually, neutrinos are produced together with charged leptons (e or μ). Therefore, two or more charged leptons in an event implies that there might be more than one neutrino missing, in which case we cannot assume that the missing mass is close to zero. For this reason, we select events with only one identified lepton. Leptons are required to have $p^{\rm Lab} > 0.8$ GeV/c. This requirement helps reduce backgrounds from hadrons misidentified as leptons and random combinations of leptons and D mesons.

For hadronic event selection, we require that each event have at least 5 well-reconstructed charged tracks, a total visible energy of at least 0.15 times the center-of-mass (CM) energy and an event vertex that is consistent with the known interaction point. Continuum background events are suppressed by requiring the normalized 2nd Fox-Wolfram moment (R_2) [11] to be less than 0.4. For those events surviving the single-lepton event selection, this cut removes 19% of the continuum events while keeping 99% of the signal.

The D^+ candidates are reconstructed in the $D^+ \to K^-\pi^+\pi^+$ decay channel. Kaons are required to be positively identified by the hadron identification devices described in Sec. II. In addition, we require kaons not to be positively identified as either a lepton or a proton. If a charged particle is not positively identified as a lepton, kaon, or proton, we treat it as a pion. The three charged tracks in the $K^-\pi^+\pi^+$ candidate are then kinematically fit to a D^+ decay vertex and we require that the impact parameter of each track with respect to the vertex location be consistent with zero.

We also impose a cut on P_{D^+} in order to suppress feed-down background from $B \to D^*\ell\nu$, etc. In Fig. 1, we show several MC distributions of P_{D^+} (at the generator level) for various sources of D^+ production: from $\bar{B}^0 \to D^+\ell^-\bar{\nu}$ (top), from $\bar{B}^0 \to D^{*+}\ell^-\bar{\nu}$ (middle) and from other B decays (bottom). We require $1.0 < P_{D^+} < 2.5$ GeV/c. The low side limit provides a substantial suppression of feed-down background and the high side limit is effective in suppressing continuum background. The momentum requirement removes 44% of $B\bar{B}$ background, 29% of continuum background while retaining 96% of the $\bar{B}^0 \to D^+\ell^-\nu$ signal. Figure 2 shows the D^+ candidate invariant mass distribution for events satisfying the above-mentioned selection criteria. We select $K\pi\pi$ combinations where the invariant mass is within 3σ of the nominal D^+ mass.

To reduce the feed-down background from $B \to D^{*+}\ell\nu$ decays, we reject D^+ candidates that are consistent with being produced in the decay $D^{*+} \to D^+\pi^0$. We select π^0 mesons by requiring that the two photon invariant mass is within 3σ of the nominal π^0 mass, where the energy of each photon is required to be greater than 20 MeV. We calculate the mass difference $M_{K^-\pi^+\pi^+\pi^0} - M_{K^-\pi^+\pi^+}$ and if it is within 3σ of the nominal value for a D^{*+} decay, that D^+ candidate is vetoed. This removes 38% of D^{*+} feed-down background while retaining 96% of $\bar{B}^0 \to D^+\ell^-\nu$ signal.

Using the hermeticity of the Belle detector, we extract information on the neutrino from the missing momentum and energy in each event. In the center of mass frame, the total momentum of the system is zero, and the total energy is the sum of the two beam energies. The missing energy, momentum and missing mass are calculated as follows:

$$E_{\rm miss} = 2E_{\rm beam} - \Sigma E_i,$$
$$\vec{p}_{\rm miss} = -\Sigma \vec{p}_i,$$
$$M^2_{\rm miss} = E^2_{\rm miss} - p^2_{\rm miss},$$

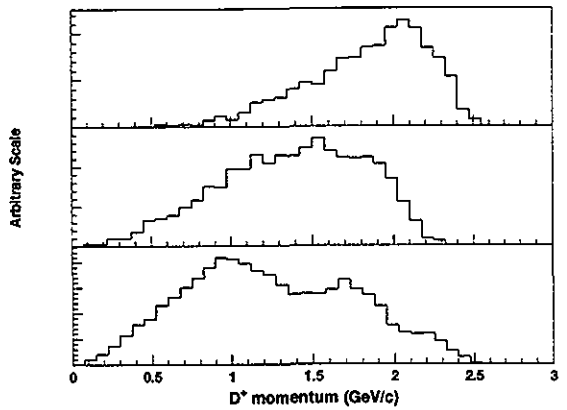

FIG. 1. The MC event-generator D^+ momentum distributions in the $\Upsilon(4S)$ rest frame. The top histogram is for D^+ from $B \to D^+\ell\nu$, the middle for $B \to D^*\ell\nu$, and the bottom for other B decays.

where the sum is over all reconstructed particles i in the event. If the only undetected particle in an event is a neutrino, the missing momentum and energy can be attributed to the neutrino in which case the missing mass should be consistent with zero.

In calculating the missing energy and momentum, we identify each charged particle using the lepton and hadron identification devices. We also add the neutral showers recorded in the ECL that are not matched to any charged track. Moreover, we require that the shower shape is consistent with that of a photon and the deposited energy is greater than 30 MeV for the barrel region and 50 MeV for the endcap.

For the $E_{\rm miss}$ and $\vec{p}_{\rm miss}$ measurements, it is crucial to reconstruct all the particles produced in the event. Since the initial state is charge-neutral, we should have a net charge of zero if we detect all the particles and nothing extra. Hence, we require that the net charge, ΔQ in the event should be close to zero to reject events with other missing charged particles. In Table I, we compare the effects of a $|\Delta Q|$ requirement on the resolution of the missing momentum for signal MC. In this table, the resolution and shift values are obtained by fitting the distribution of $\vec{p}_{\rm miss} - \vec{p}_\nu$ with a Gaussian shape, where $\vec{p}_\nu$ is the generated momentum 3-vector of the signal neutrino. In the MC, 81% (77%) of signal (background) events survive

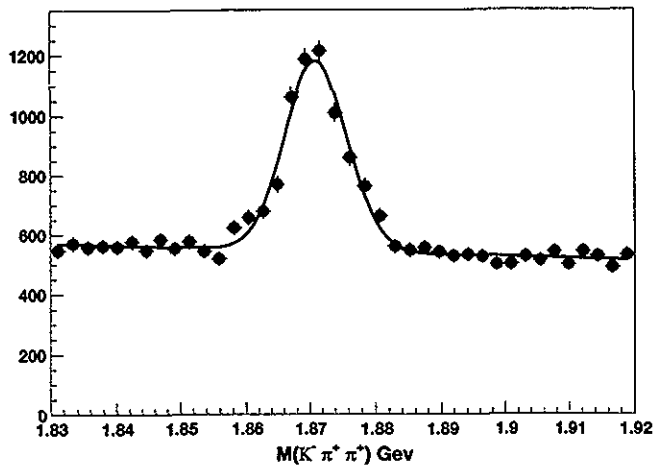

FIG. 2. The invariant mass distribution for $D^+ \to K^-\pi^+\pi^+$ candidates, fitted to a Gaussian signal plus a linear background function.

$|\Delta Q| \leq 1$ requirement, while 41% (36%) of signal (background) events satisfy $\Delta Q = 0$. Moreover, the $\vec{p}_{\rm miss}$ resolution for $\Delta Q = 0$ events is not significantly better than that for $|\Delta Q| = 1$ events, hence we select events with $|\Delta Q| \leq 1$.

Sometimes a particle escapes the Belle detector and leaves undetected energy and momentum in the event. Most often this happens when the missing particle (not necessarily a neutrino) goes down the beampipe. To reject the events with such missing particles making significant contributions to $E_{\rm miss}$ and $\vec{p}_{\rm miss}$, we require $|\cos\theta_{\vec{p}_{\rm miss}}| < 0.9$ in the CM frame. The MC simulation shows that 88% (86%) of signal (background) events pass this cut.

A variable $\cos\theta_{B-D\ell}$ is defined as the cosine of the angle between $\vec{p}_{B^0}$ and $\vec{p}_{D^+\ell^-}$(= $\vec{p}_{D^+} + \vec{p}_{\ell^-}$), and it satisfies the following kinematic relation:

$$\cos\theta_{B-D\ell} = \frac{2E_B E_{D\ell} - M_B^2 - M_{D\ell}^2}{2|\vec{p}_B||\vec{p}_{D\ell}|}. \qquad (2)$$

Figure 3 shows the $\cos\theta_{B-D\ell}$ distribution. The top figure shows the on-resonance data (points with error bars) with generic $B\bar{B}$ MC overlayed, and the bottom figure shows the signal MC. In making these plots, the event selection procedures up to D^+ reconstruction and the corresponding invariant mass cut are imposed. The signal events are mostly distributed within the physically allowed region $|\cos\theta_{B-D\ell}| < 1$, while the background events extend to a much wider range. We require that candidates have $|\cos\theta_{B-D\ell}| < 1$.

TABLE I. Effects of $|\Delta Q|$ cut on the $\vec{p}_{\rm miss}$ resolution for signal MC

	$\|\Delta Q\| \leq 1$	no requirement
resolution (MeV)	469±18	487±17
shift (MeV)	164±19	195±18

TABLE II. Summary of efficiencies and S/N ratio after all cuts. ($\bar{B}^0 \to D^+\ell^-\bar{\nu}$ mode)

channel	S/N	efficiency
μ^-	1.149	2.159%
e^-	1.148	2.258%

Since we expect the missing decay products in signal events to be consistent with a single neutrino, we impose the requirement that the missing mass of the event should be close to zero. Therefore, we require $-2.0 < M^2_{\rm miss} < 3.0$ GeV$^2/c^4$. Figure 4 shows the $M^2_{\rm miss}$ distributions for data (points with error bars) and MC events (open histogram).

Since the resolution of the momentum measurement is better than that of energy, we take $(E_\nu, \vec{p}_\nu) = (|\vec{p}_{\rm miss}|, \vec{p}_{\rm miss})$ as the 4-momentum of the neutrino. Combining the energy-momentum 4-vectors for the reconstructed D^+ meson, the signal lepton and the neutrino, and using the constraint of energy-momentum conservation, we obtain the variables for full B decay reconstruction, *i.e.* the beam constrained mass $M_{\rm B}$ and the energy difference ΔE defined as below:

$$\Delta E = E_{\rm beam} - (E_{D^+} + E_{l^-} + E_\nu), \tag{3}$$

$$M_{\rm B} = \sqrt{E^2_{\rm beam} - |\vec{p}_{D^+} + \vec{p}_{l^-} + \alpha\vec{p}_\nu|^2}. \tag{4}$$

We select events with ΔE close to 0, by requiring $-0.2 < \Delta E < 1$ (GeV) and impose that condition $\Delta E = 0$ with $\alpha = 1 + \Delta E/E_\nu$ as shown in the Eq. 4, in the calculation of $M_{\rm B}$.

After all cuts are applied, we measure the yield in the $M_{\rm B}$ signal region defined as $M_{\rm B} > 5.24$ GeV/c^2. Figure 5 shows the $M_{\rm B}$ distributions after all other event selection criteria. The points with error bars represent on-resonance data. Here the combinatoric background is already subtracted. Also displayed in the figure are various background components. Table II shows the signal efficiency and the corresponding signal-to-background (S/N) ratio after all cuts are applied. In calculating the S/N ratio in Table II, it is assumed that $\mathcal{B}(\bar{B}^0 \to D^+\ell^-\nu) = 2\%$.

Table III lists the number of signal events and estimated backgrounds in the signal region, after all event selection criteria are applied. Using the signal efficiency $\epsilon = 2.21\%$ and sub-decay branching ratio $\mathcal{B}(D^+ \to K^-\pi^+\pi^+) = 9.0\%$ [15], we obtain the branching ratio $\mathcal{B}(\bar{B}^0 \to D^+\ell^-\bar{\nu}) = (2.07 \pm 0.21)\%$, where the error is statistical only.

TABLE III. The number of signal and backgrounds in the signal region after all event selection criteria are applied. ($\bar{B}^0 \to D^+\ell^-\bar{\nu}$ mode)

total yield	431±20.8
combinatoric	121±11.0
correlated	60.1
uncorrelated	7.5
continuum	5.9
fake lepton	7.0±0.48
Signal Events	229.5±23.5

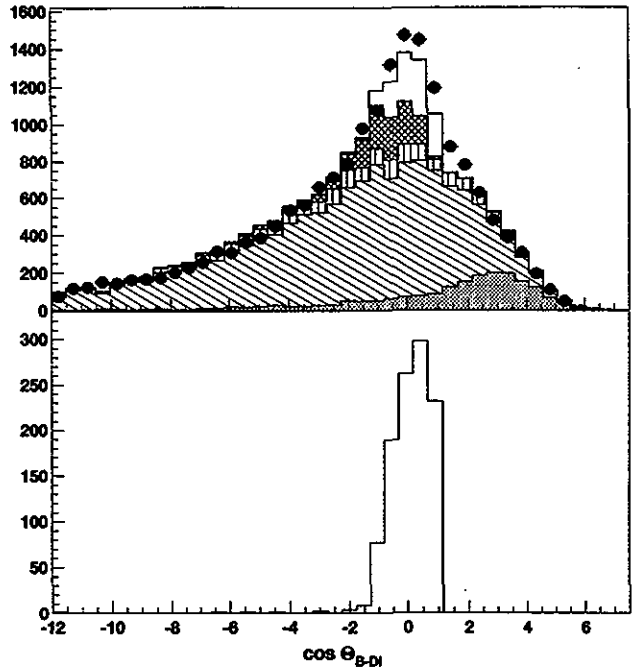

FIG. 3. The $\cos\theta_{B-D\ell}$ distributions (top) for data (points with error bar)and MC events (histogram) and (bottom) for $\bar{B}^0 \to D^+\ell^-\bar{\nu}$ signal MC events. The shaded component is the continuum and fake lepton background, the hatched histogram is the combinatoric background, the vertical hatched histogram is the uncorrelated background, and the crosshatched histogram shows the correlated background.

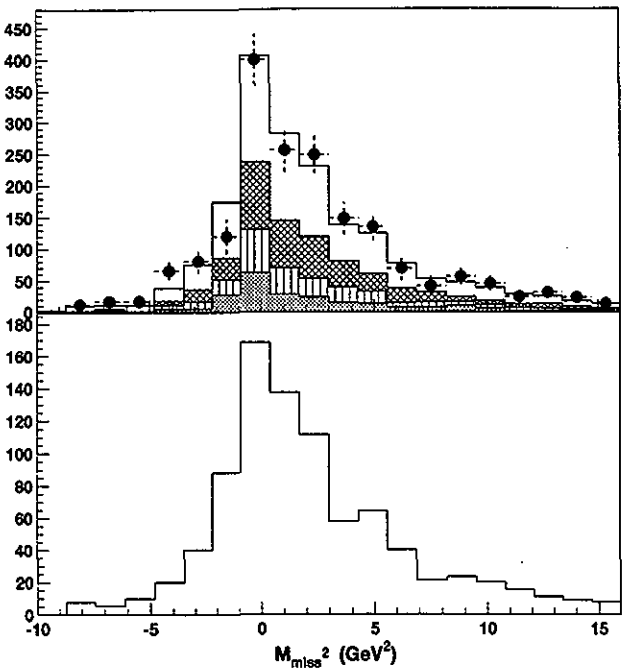

FIG. 4. $M^2_{\rm miss}$ distributions (top) for data (points with error bar)and MC events (histogram) and (bottom) for $\bar{B}^0 \to D^+\ell^-\bar{\nu}$ signal MC events. The histogram shading and normalization is the same as that in FIG. 3.

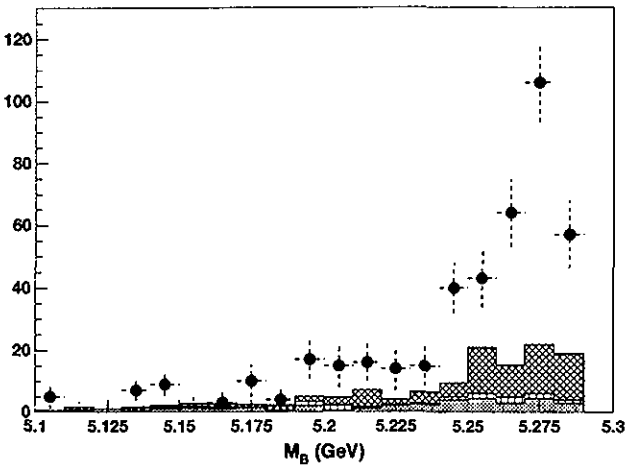

FIG. 5. The $M_{\rm B}$ distribution and MC predicted backgrounds for the $\bar{B}^0 \to D^+\ell^-\bar{\nu}$ mode. The points with error bars show the sideband and fake lepton subtracted data and the MC predicted backgrounds are shown as the histograms (shaded with the same convention as FIG. 3).

C. The $\bar{B}^0 \to D^{*+}\ell^-\bar{\nu}$ mode

We study the $\bar{B}^0 \to D^{*+}\ell^-\bar{\nu}$ ($\ell = e, \mu$) decay mode using the subsequent decays $D^{*+} \to D^0\pi^+$ and $D^0 \to K^-\pi^+$ or $D^0 \to K^-\pi^+\pi^0$. We require the same hadronic event selection criteria as described in Sec. III B. To suppress background from $e^+e^- \to q\bar{q}$ continuum events, the same cut on the 2nd Fox-Wolfram moment ($R_2 < 0.4$) as described in Section III B is applied.

Each event is required to contain at least one electron candidate with the CM momentum p_ℓ in the range between 1.0 GeV/c and 2.45 GeV/c, or at least one muon candidate with CM momentum in the range between 1.4 GeV/c and 2.45 GeV/c. Hadrons are identified using the same method as described in Section III B. Candidate π^0 mesons are detected using pairs of neutral clusters detected in the ECL that are consistent with being a photon and not matched to any charged track.

After identifying the particles, we search for D^0 signals in the modes $D^0 \to K^-\pi^+$ and $D^0 \to K^-\pi^+\pi^0$. In the first mode, after a $K^-\pi^+$ combination is selected, we use kinematic fitting to find the $K^-\pi^+$ vertex position and the momentum vector of each particle is recalculated after the fitting. In order to select events with well reconstructed D^0 decay vertices for $K^-\pi^+$ candidates, the impact parameter of each daughter particle was required to be less than 0.5 cm with respect to the vertex position.

For the three-body D decay, we first find the vertex position by using only the $K^-\pi^+$ tracks in the kinematic fitting, then this vertex position is used in a D^0 mass constraint fit that includes the π^0. A similar requirement on the impact parameter of the $K^-\pi^+$ tracks is also imposed. The $D^0 \to K^-\pi^+$ candidates must have a $K^-\pi^+$ invariant mass within 3σ of the nominal D^0 value. The mean and width of the $K^-\pi^+$ invariant mass peak in the data are 1.865 GeV/c^2 and 6.2 MeV/c^2, respectively, and are consistent with the Monte Carlo.

Next we combine D^0 candidates with charged pion candidates to fully reconstruct the D^{*+} meson in the mode $D^{*+} \to D^0\pi^+$. We call this additional pion the slow pion (π_s) because its momentum is less than 225 MeV/c in the $\Upsilon(4S)$ CM frame. To improve the resolution of the mass difference ($\delta m = M_{K\pi\pi_s} - M_{K\pi}$ or $M_{K\pi\pi^0\pi_s} - M_{K\pi\pi^0}$), the $D^0 - \pi_s^+$ vertex is fitted using the position information of the interaction point (IP). Figure 6 shows the δm distribution. The peak value of the mass difference is 145.4 MeV/c^2 and the corresponding width is approximately 400 keV/c^2. We select D^{*+} candidates in both channels by requiring that δm be within 2 MeV/c^2 of the peak value. The momentum of D^{*+} candidates must satisfy $|P_{D^*}|/\sqrt{E_B^2 - M_{D^*}^2} < 0.5$ to be consistent with coming from a B decay. We also kinematically fit the D^0-lepton vertex, and the lepton momentum vector is recalculated requiring that the lepton track originates at this new vertex.

Similar to the previous section, we have a missing neutrino in the final state and we use missing energy and momentum to extract the information on the neutrino. In this analysis, however, we use the information on the missing neutrino only to require consistency by making a loose cut on $M_{\rm B}$. For signal events, we expect $M_{\rm miss}^2 = M_\nu^2 = 0$, where in the event CM frame

$$M_{\rm miss}^2 \equiv (P_B - P_{D^*\ell})^2 = M_B^2 + M_{D^*\ell}^2 - 2E_B E_{D^*\ell} + 2|\vec{P}_B||\vec{P}_{D^*\ell}|\cos\theta_{B,D^*\ell}. \qquad (5)$$

Here P_B and $P_{D^*\ell}$ are 4-vectors, while $\vec{P}$ denotes 3-vectors. Although the angle $\theta_{B,D^*\ell}$ between the B and $(D^{*+} + \ell)$ momentum direction is unknown, one can neglect the last

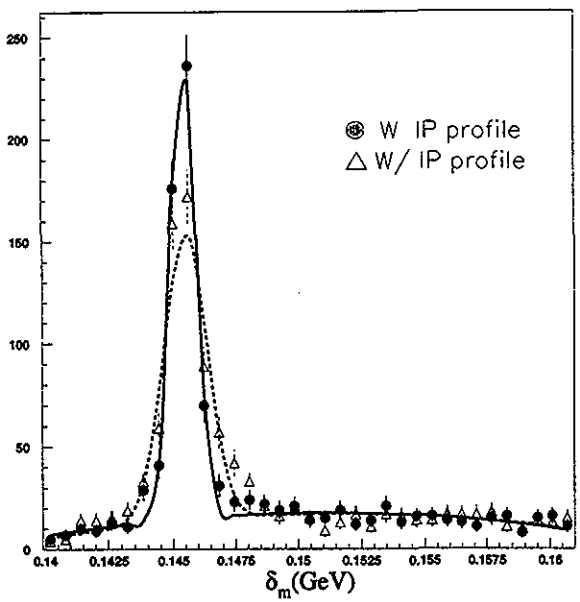

FIG. 6. The δm distribution. The solid circles represent the distribution after slow pion vertexing using the IP profile information while the open triangles show the distribution without including the slow pion in the vertex.

term since the B meson is produced almost at rest. Thus we obtain:

$$M^2_{\rm miss} = M^2_B + M^2_{D^*\ell} - 2E_B E_{D^*\ell}$$

A cut on $M^2_{\rm miss}$ is effective to suppress the $\bar{B} \to D^{**}\ell\bar{\nu}$ decays, hence we require $M^2_{\rm miss} < 1.0$. The quantity $\cos\theta_{B,D^*\ell}$ is highly correlated with $M_{\rm miss}$, nevertheless we impose the kinematic consistency condition with the requirement $|\cos\theta_{B,D^*\ell}| < 1$. Figure 7 shows the $\cos\theta_{B,D^*\ell}$ distribution for signal MC events, generic $B\bar{B}$ MC events, and continuum MC events.

By attributing the missing energy and momentum to the undetected neutrino and using the fact that the sum of energies of the B decay products in the CM frame is equal to the beam energy, $M_{\rm B}$ is calculated as follows:

$$M_B = \sqrt{E^2_{beam} - |\vec{P}_{D^*} + \vec{P}_\ell + \vec{P}_\nu|^2}\,,$$

where $\vec{P}_\nu$ is obtained from missing momentum as in Sec. III B. We require $M_B > 5.0$ GeV/c^2.

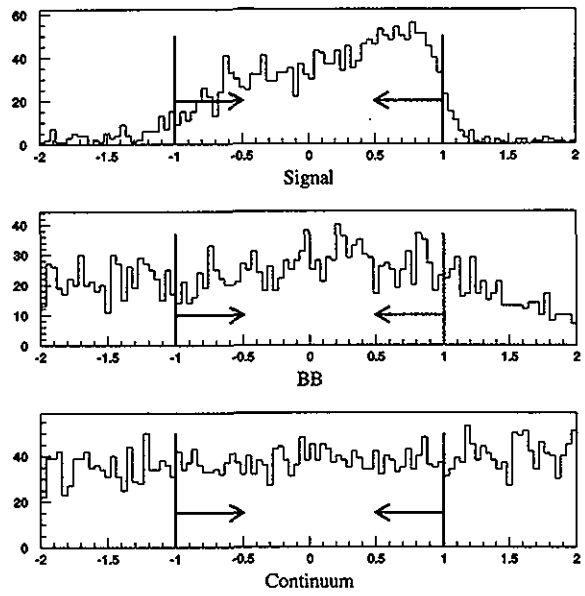

FIG. 7. Cosine of the angle between B and $D^*\ell$ direction in MC: the top figure is for the signal MC events, the middle plot is for generic $B\bar{B}$ MC events, and the bottom one is for continuum MC events.

The reconstruction efficiencies for $\bar{B}^0 \to D^{*+}\ell^-\bar{\nu}$ decays are calculated using a MC event sample that is processed through the full detector simulation and reconstruction, and corrected for data/MC differences in hadron and lepton identification. The track-finding efficiency is checked with real data by comparing $\eta \to \pi^+\pi^-\pi^0$ and $\eta \to \gamma\gamma$ decays. Table IV shows the signal efficiency values for four separate subsamples. The values do not include sub-decay branching fractions. Table V shows the number of events in the signal region as well as the estimated backgrounds after all event selection criteria are imposed. The numbers are displayed separately for each subsample of the analysis.

The signal yield is determined using the 2-dimensional distribution of C vs. $M^2_{\rm miss}$, where C is the coefficient of $\cos\theta_{B,D^*\ell}$ in Eq. 5 *i.e.* $C = 2|\vec{P}_B||\vec{P}_{D^*\ell}|$. Figure 8 shows a scatter plot of C vs. $M^2_{\rm miss}$ for real data, while the four plots in Fig. 9 correspond to signal MC and generic $B\bar{B}$ MC events. In each plot, the signal region is inside a triangle that is the kinematic boundary determined by Eq. 5 [14]. Combining the results of the

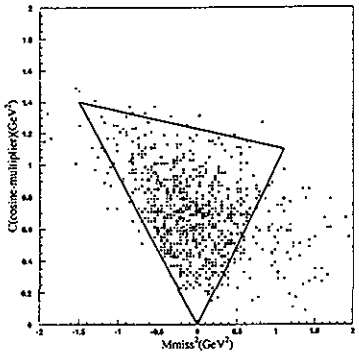

FIG. 8. Distribution of C vs. $M^2_{\rm miss}$ for on-resonance data. The signal region for $\bar{B}^0 \to D^{*+}\ell^-\bar{\nu}$ decay is inside the triangle.

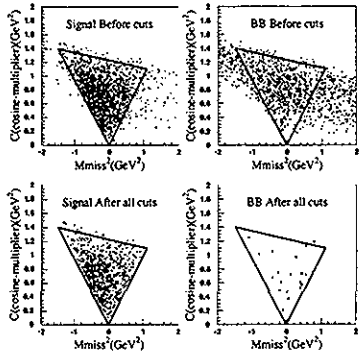

FIG. 9. MC distributions of C vs. $M^2_{\rm miss}$ for signal and generic $B\bar{B}$ events, before (top) and after (bottom) final event selection.

TABLE IV. Efficiency for each mode where the error contains the systematic uncertainties.

Mode	$K^-\pi^+$ (e^-)	$K^-\pi^+$ (μ^-)	$K^-\pi^+\pi^0$ (e^-)	$K^-\pi^+\pi^0$ (μ^-)
efficiency (%)	5.6± 0.39	4.8± 0.43	1.0± 0.07	0.97± 0.09

four sub-decay modes weighted by their statistical errors, we obtain the branching ratio $\mathcal{B}(\bar{B}^0 \to D^{*+}\ell^-\bar{\nu}) = 4.74 \pm 0.25$ (%), where the error is statistical only.

IV. SYSTEMATIC UNCERTAINTIES

In the $\bar{B}^0 \to D^+\ell^-\bar{\nu}$ analysis, the systematic uncertainties are studied separately for additive and multiplicative terms. The additive terms are related to the background estimation while the multiplicative terms are related to obtaining the signal yield and the efficiency.

For systematic errors related to the signal efficiency, we consider uncertainties in the efficiency of the D^+ reconstruction with the single lepton condition, hadron identification efficiency, the number of $B\bar{B}$ pairs, and the $D^+ \to K^-\pi^+\pi^+$ branching fraction. Summing these uncertainties in quadrature, the relative uncertainty ($\delta\mathcal{B}/\mathcal{B}$) in the branching ratio measurement is 11.2% (see Table VI).

Since we rely on MC simulation to estimate the correlated backgrounds, we vary the relative fractions of $D^{**}\ell\nu$ and $D\pi\ell\nu$ within the constraint of the measured inclusive semileptonic branching fraction [16] and estimate that the relative error due to correlated background is 7.8%. Because of a substantial correlation in the charge and momentum between the D^+ and ℓ^-, the amount of uncorrelated background is small. Similarly, background from the continuum is very small. Hence, even assuming large uncertainties in these backgrounds

TABLE V. Summary of the signal yield and background estimation for the $\bar{B}^0 \to D^{*+}\ell^-\bar{\nu}$ mode.

Mode	$K^-\pi^+(e^-)$	$K^-\pi^+(\mu^-)$	$K^-\pi^+\pi^0(e^-)$	$K^-\pi^+\pi^0(\mu^-)$
Raw yield	203 ± 14.2	154±12.4	162 ± 12.7	128±11.3
Combinatoric	26 ± 3.7	16 ± 2.7	46 ± 6.2	32 ± 5.4
Correlated	4	2	5	3
Uncorrelated	2	1	1	0
Lepton fake	1	1.7	0.8	1.4
Continuum	1	0	1	0
Net yield	169±14.7	133±12.7	108 ± 14.2	92 ± 12.5

TABLE VI. Summary of relative systematic errors ($\Delta\mathcal{B}/\mathcal{B}$) on the $\mathcal{B}(\bar{B}^0 \to D^+\ell^-\bar{\nu})$ measurement.

multiplicative systematic uncertainty (%)	
D^+ & single lepton requirement	8.7
hadron ID effi. correction	2.1
Number of $B\bar{B}$ events	1.0
$\mathcal{B}(D^+ \to K^-\pi^+\pi^+)$	6.7
additive systematic uncertainty (%)	
correlated background	7.8
other background	0.9
MC adjustment study	5.8
total	15.0

makes a negligible difference in our result. We vary the lepton misidentification probability by 25% from its nominal value and find that the systematic uncertainty is less than 1%.

To assess the uncertainties in our MC simulation, we vary several performance-related parameters in our simulation including the track-finding efficiency, track momentum resolution, photon finding efficiency and energy resolution. Summing each deviation from the standard analysis result in quadrature gives a relative uncertainty of 5.8%.

The resulting relative systematic errors in the measurement of $\mathcal{B}(\bar{B}^0 \to D^+\ell^-\bar{\nu})$ are summarized in Table VI.

For the $\bar{B}^0 \to D^{*+}\ell^-\bar{\nu}$ analysis, we estimate the systematic errors separately for different sub-decay modes. However, some systematic uncertainties are common to all four sub-decay modes while others are common to two sub-decay modes; in such cases, we use the common values for systematic uncertainties.

The possible sources of multiplicative systematic uncertainties in this mode are : lepton and hadron identification efficiencies, track-finding efficiencies, slow-π efficiency for D^* reconstruction, number of $B\bar{B}$ pairs in the event sample and the sub-decay branching ratios. As in the $D^+\ell\nu$ mode, the systematic uncertainties related to background estimation are

TABLE VII. Summary of relative systematic errors on the $\mathcal{B}(\bar{B}^0 \to D^{*+}\ell^-\bar{\nu})$ measurement.

	$K^-\pi^+e^-$	$K^-\pi^+\mu^-$	$K^-\pi^+\pi^0e^-$	$K^-\pi^+\pi^0\mu^-$
Error Source	$\Delta\mathcal{B}/\mathcal{B}$(%)			
N($B\bar{B}$)	1.0			
$\mathcal{B}(D^{*+} \to D^0\pi^+)$	2.0			
Tracking reconstruction efficiency	3.7			
Kaon identification efficiency	4.0			
Slow pion efficiency	4.4			
Subtotal for common sys. err.	7.5			
$\mathcal{B}(D^0$ decay)	2.3		6.5	
Lepton identification efficiency	2.0	5.0	2.0	5.0
Variation of cuts	0.9	1.1	1.0	1.1
Combinatoric background	1.7	2.3	3.7	3.2
Correlated background	3.6	2.3	4.6	4.3
Other background & fake leptons	2.9	2.2	2.7	4.3
Subtotal for non-common sys. err.	5.86	6.83	9.45	10.8

also considered. In addition, we vary the event selection criteria and take the deviation from the standard result as another source of systematic uncertainty.

The resulting relative systematic errors in the $\mathcal{B}(\bar{B}^0 \to D^{*+}\ell^-\bar{\nu})$ measurement are summarized in the Table VII. If we calculate the weighted average as described in Section III C, the combined relative systematic error is 10.7%.

V. SUMMARY

From the results in Sections III and IV, we obtain the following preliminary exclusive B semileptonic branching fractions:

$$\mathcal{B}(\bar{B}^0 \to D^+\ell^-\bar{\nu}) = 2.07 \pm 0.21 \pm 0.31\ (\%)$$
$$\mathcal{B}(\bar{B}^0 \to D^{*+}\ell^-\bar{\nu}) = 4.74 \pm 0.25 \pm 0.51\ (\%)$$

where the first error is statistical and the second one is systematic for both measurements. These results are consistent with existing measurements. [14,17]

We have shown that information on an undetected single neutrino can be reliably extracted by kinematic constraints with the Belle detector. With more data which will be accumulated soon, we will apply this method to make precise measurements of the CKM matrix elements V_{cb} and V_{ub}.

ACKNOWLEDGEMENTS

We gratefully acknowledge the efforts of the KEKB group in providing us with excellent luminosity and running conditions and the help with our computing and network systems provided by members of the KEK computing research center. We thank the staffs of KEK and collaborating institutions for their contributions to this work, and acknowledge support from the Ministry of Education, Science, Sports and Culture of Japan and the Japan Society for the Promotion of Science; the Australian Research Council and the Australian Department of Industry, Science and Resources; the Department of Science and Technology of India; the BK21 program of the Ministry of Education of Korea and the Basic Science program of the Korea Science and Engineering Foundation; the Polish State Committee for Scientific Research under contract No.2P03B 17017; the Ministry of Science and Technology of Russian Federation; the National Science Council and the Ministry of Education of Taiwan; the Japan-Taiwan Cooperative Program of the Interchange Association; and the U.S. Department of Energy.

REFERENCES

[1] N. Cabibbo, Phys. Rev. Lett. **10**, 531 (1963); M. Kobayashi and T. Maskawa, Prog. Theor. Phys. **49**, 652 (1973)

[2] N. Isgur and M. B. Wise, Phys. Lett. **B232**, 113 (1989); M. Neubert, Phys. Rep. **245**, 259 (1994).

[3] KEKB accelerator group, KEKB B Factory Design Report, KEK Report 95-7, 1995.

[4] BELLE Collaboration, Technical Design Report, KEK Report 95-1, 1995.

[5] G. Alimonti *et al.*, KEK preprint 2000-34.

[6] H. Hirano *et al.*, KEK Preprint 2000-2, submitted to Nucl. Inst. Meth.; M. Akatsu *et al.*, DPNU-00-06, submitted to Nucl. Inst. Meth.

[7] T. Iijima *et al.*, Proceedings of the 7th International Conference on Instrumentation for Colliding Beam Physics, Hamamatsu, Japan, Nov 15-19, 1999.

[8] H. Kichimi *et al.*, submitted to Nucl. Inst. Meth.

[9] H. Ikeda *et al.*, Nucl. Inst. Meth. **441**, 401 (2000).

[10] A. Abashian *et al.* ,Nucl. Instr. Meth. **A449**, 112 (2000).

[11] G. Fox and S. Wolfram, Phys. Rev. Lett. **41**, 1581 (1978)

[12] N. Isgur and D. Scora, Phys. Rev. **D52**, 2783 (1995); N. Isgur, D. Scora, B. Grinstein, and M. B. Wise, Phys. Rev. **D39**, 799 (1989).

[13] CLEO Collaboration, J. P. Alexander *et al.*, Phys. Rev. Lett. **77**, 5000 (1996).

[14] CLEO Collaboration, B. Barish *et al.*, Phys. Rev. **D51**, 1014 (1995).

[15] C. Caso *et al.* (Particle Data Group), Eur. Phys. Jour. **C3**, 1 (1998).

[16] CLEO Collaboration, B. Barish *et al.*, Phys. Rev. Lett. **76**, 1570 (1996).

[17] CLEO Collab., J. Bartelt *et al.*, Phys. Rev. Lett. **82** 3746 (1999); OPAL Collab., K. Ackerstaff *et al.*, Phys. Lett. **B395**, 128 (1997); CLEO Collab., M. Athanas *et al.*, Phys. Rev. Lett. **79**, 2208 (1997); ALEPH Collab., D. Buskulic *et al.*, Phys. Lett. **B395**, 373 (1997); DELPHI Collab., P. Abreu *et al.*, Z. Phys. **C71**, 539 (1996); ARGUS Collab., H. Albrecht *et al.*, Phys. Lett. **B324**, 249 (1994); ARGUS Collab., H. Albrecht *et al.*, Phys. Lett. **B229**, 175 (1989).